Open access • Journal Article • DOI:10.1109/JSTARS.2019.2896923

Evaluation of Machine Learning Algorithms in Spatial Downscaling of MODIS Land Surface Temperature — Source link

Wan Li, Li Ni, Zhao-Liang Li, Si-Bo Duan ...+1 more authors

Institutions: Chinese Academy of Sciences

Published on: 01 Mar 2019 - IEEE Journal of Selected Topics in Applied Earth Observations and Remote Sensing (IEEE)

Topics: Artificial neural network and Support vector machine

Evaluation of Machine Learning Algorithms in Spatial Downscaling of MODIS Land Surface Temperature

Wan Li, Li Ni, Hua Wu, Zhao-Liang Li, Si-Bo Duan

Evaluation of Machine Learning Algorithms in Spatial Downscaling of MODIS Land Surface Temperature

Wan Li, Li Ni, Hua Wu, Zhao-Liang Li and Si-Bo Duan

Abstract—**Land surface temperature is described as one of the most important environmental parameters of the land surface biophysical process. Commonly, the remote sensed LST products yield a tradeoff between high temporal and high spatial resolution. Thus, many downscaling algorithms have been proposed to address this issue. Recently, downscaling with machine learning algorithms, including artificial neural networks (ANN), support vector machine (SVM) and random forest (RF) and so on, have gained more recognition with fast operation and high computing precision. This paper intends to make a comparison between machine learning algorithms to downscale the LST product of the Moderate Resolution Imaging Spectroradiometer (MODIS) from 990 m to 90 m, and downscaling results would be validated by the resampled LST product of the Advanced Spaceborne Thermal Emission and Reflection Radiometer (ASTER). The results are further compared with the classical algorithm-thermal sharpening algorithm (TsHARP), using images derived from two representative kind of areas of Beijing City. The result shows that: (1) All machine learning algorithms produce higher accuracy than TsHARP. (2) The performance of TsHARP on urban area is unsatisfactory than rural because of the weak indication of impervious surface by NDVI, however, machine learning algorithms get the desired results on both two areas by importing more explanatory factors, such as reflectance, spectral indices and terrain factors, to depict the spatial distribution of LST comprehensively. (3) Additionally, machine learning algorithms are promising to achieve a universal framework which can downscale LST for any area within the training data from long spatiotemporal sequences.**

Index Terms—**Land surface temperature, downscaling, machine learning, comparison**

This work was supported by the National Key R&D Program of China under Grant No. 2018YFB0504800, by the Strategic Priority Research Program of Chinese Academy of Sciences under Grant No. XDA20030302, and by the National Natural Science Foundation of China under Grant No. 41771398 and No. 41871267. (Corresponding author: Hua Wu.)

W. Li is with the State Key Laboratory of Resources and Environment Information System, Institute of Geographic Science and Nature Resources Research, Chinese Academy of Sciences, Beijing 100101, China, and also with University of Chinese Academy of Sciences, Beijing 100049, China (e-mail: liwan16@mails.ucas.ac.cn).

L. Ni is with Key Laboratory of Digital Earth Science, Institute of Remote Sensing and Digital Earth, Chinese Academy of Sciences, Beijing 100094, China (e-mail: nili@radi.ac.cn).

H. Wu is with the State Key Laboratory of Resources and Environment Information System, Institute of Geographic Science and Nature Resources Research, Chinese Academy of Sciences, Beijing 100101, China, with University of Chinese Academy of Sciences, Beijing 100049, China, and also with Jiangsu Center for Collaborative Innovation in Geographical Information Resource Development and Application, Nanjing 210023, China (e-mail: wuhua@igsnrr.ac.cn).

S.-B. Duan is with the Key Laboratory of Agri-Informatics, Ministry of Agriculture/Institute of Agricultural Resources and Regional Planning, Chinese Academy of Agricultural Sciences, Beijing 100081, China (e-mail: duansibo@caas.cn).

Z.-L. Li is with the Key Laboratory of Agri-informatics, Ministry of Agriculture Institute of Agricultural Resources and Regional Planning, Chinese Academy of Agricultural Sciences, Beijing 100081, China, and also with ICube, UdS, CNRS, 67412 Illkirch, France (e-mail: lizhaoliang@caas.cn).

I. Introduction

LAND surface temperature (LST), described as one of the most important environmental parameters of the interaction of land surface and atmosphere, water circulation as well as energy exchange within the regional or global scale, has played an essential role on the research of evapotranspiration, urban heat island effects and global warming [1]. A finer resolution LST has been widely used in hydrological equilibrium assessment, global warming study, urban heat island effect assessment as well as surface evapotranspiration calculation [2]. Commonly, the existing land surface temperature products are mostly derived from the thermal infrared remote sensing image, with the superiority of repeated and continuous observation to surface. However, because of the heterogeneity of most surface parameters such as land cover types and the physical and thermal properties of soil moisture, the thermal infrared images from satellite sensors always have relatively lower resolution, the detailed spatial information cannot be efficiently captured from lower resolution LSTs during a revisiting cycle [3]. This issue hindered the research of land surface temperature retrieval and application; hence an effective downscaling algorithm is desperately needed to provide high quality temperature products [4].

During the past few years, many efforts have been tried to advance the spatial downscaling algorithms of satellite-based land surface temperature datasets based on the relationship between LST and other land surface characteristics, which can be roughly divided into three categories based on mechanism: (1) Statistical regression algorithm-based algorithm; (2) Modulation distribution-based algorithm; (3) Linear spectral mixture model-based algorithm [5-8]. Among these methods the statistical regression algorithm has been commonly accepted as the easy-manipulative and the satisfactory accuracy, thus many scholars have carried out research on spatial downscaling based on this field. The early regression algorithms tend to focus on the statistical relationship between vegetation indices and LST, such as normalized difference vegetation index (NDVI), fractional vegetation cover and soil-adjusted vegetation index (SAVI). Other remote sensing indices, such as normalized difference building index (NDBI) and normalized difference dust index (NDDI) and so on, have been applied to downscaling researches under different circumstances [9-11]. Recent studies also addressed the issues on the linear or nonlinear regression algorithms between LST and these remote sensing indices, including the geographically weighted regression model, the regression-kriging model and Bayesian-based model [12-14]. The machine learning algorithms, such as artificial neural network (ANN), support vector machine (SVM), the combination of global window and moving window regression trees as well as random forest (RF), have gotten great accuracies in fitting the nonlinear relationship between LST and other variables [15-18]. Accordingly, several researches have been carried out to compare the existing downscaling algorithms, Zhan et al. provided the review of the issue of the disaggregation of remotely sensed land surface temperature (DLST) and presented several caveats which should be emphasized in future research [19]. Bisquert et al. compared several disaggregation methods with two different sensors and proved the potential of the disaggregation techniques applied to two different sensors [20]. Bonafoni et al. evaluated different regressive downscaling schemes by using the representative spectral index (SI) and then pointed out the importance of vegetation and built-up/soil indexes in disaggregation [21].

The objectives of this paper are to evaluate the performance of three downscaling algorithms based on machine learning: ANN, SVM and RF to obtain LST product with finer resolution from the coarser resolution. Variables that have closed correlation with land surface status like vegetation coverage, topography and terrestrial radiation were introduced into model. By comparison, the strength and weaknesses of each machine learning algorithms in downscaling could be revealed. In addition, the comparison with NDVI-based algorithm, TsHARP gives the further evidence about the superiority of machine learning algorithms, which could provide guide in spatial downscaling to product LSTs with higher accuracy.

II. Methodology

A. *Study Area and Data Resources*

Figure 1 shows the spatial distribution of elevation and false color images of study areas in the paper. Two typical areas located in Beijing City were selected with different land cover types and terrains, which were marked as rural and urban area. The study areas are located at districts of Haidian and Changping in Beijing City, China. Beijing is in the northern part of North China Plain, ranging from 39°28′N to 41°05′N and from 115°25′E to 117°35′E, with the average elevation around 43.5 meters. Beijing has a typical semihumid continental monsoon climate with four clearly distinct seasons. The annual mean temperature ranges from 10°C to 12°C and mean precipitation ranging from 450 mm to 550 mm. These study areas typically contain four kinds of land cover types: vegetation, croplands, impervious surfaces (including buildings and roads) and water; study area A is mainly characterized by vegetation in the western region with undulating topography and study area B, located in the downtown area, is almost covered by impervious surfaces in the eastern regions with relatively flat topography.

The LST at finer resolution was derived from the Advanced Spaceborne Thermal Emission and Reflection Radiometer (ASTER), which is another sensor aboard the Terra satellite. The ASTER LST products (AST08), available from the NASA Earthdata Search (https://search.earthdata.nasa.gov/) with a spatial resolution of 90m, were generated from the Temperature/emissivity Separation algorithm with the accuracy of about 1.5 K [22]. The ASTER LSTs will be served as the referenced data to validate the performance of the downscaling models at the finer scale.

The LST to be downscaled is the Moderate Resolution Imaging Spectroradiometer (MODIS) LST product (MOD11A1), which was acquired on 24 July 2014 for study area A and B, MODIS is a sensor aboard the Terra satellite. MOD11A1 is available from the Land Processes Distributed Active Archive Center (LPDAAC) with the resolution of about 1 km and generated from the generalized split-window algorithm with an accuracy of about 1 K [23]. To keep the multiple relationship with the referenced ASTER LST at 90m resolution, the nearest neighbor resampling algorithm was used to resample MODIS LST product to maintain the pixel size of 990 m. Then the LST data could be downscaled from 990 to 90 m rationally.

The Landsat 8 Operational Lad Imager (OLI) image were acquired at the United States Geological Survey (USGS) Earth Resources Observation and Science (EROS) Center Science Processing Architecture with the resolution of 30m. In this study, the Landsat reflectance products with bands 2-7 and the processed spectral indices are served as the input variables for downscaling MODIS LST product from 990m to 90m.

The digital elevation model (DEM) data are derived from The NASA's Shuttle Radar Topography Mission (SRTM). The SRTM DEM data and the derivative (aspect, slope and hill-shade), with a spatial resolution of 90 m, were spatially aggregated to a resolution of 990 m by spatial averaging to the resolution of the MODIS LST for the downscaling model.

B. *Method*

1) Downscaling Methodology

In this study, the spatial downscaling algorithm is based on the relationship between LST and other land surface parameters [24]. The basic process is to construct the statistical model between LST and these predictors at coarser resolution, on the condition that the relationship is scale invariable, then the established model is applied to the study areas with finer resolution. The input variables should be intended to depict the spatial variance and continuity of LST over different regions. Therefore, this paper selects four kinds of predictor variables.

The first kind of variable is the reflectance of visible/near infrared and short-wave infrared bands derived from Landsat OLI and TIRS images, which contains much information of land cover types, land surface status and soil moisture status. Typical spectral indices indicting special land cover are also introduced to given precise instructions to study area about vegetation, water, bare land as well as impervious surface. Thirdly, terrain factors, which make a difference in the direction of solar radiation and long-wave surface cooling, have also been added in. Additionally, the land classification map was introduced as the hierarchical display of the relationship between LST and spectral patterns over different land cover types.

The specific steps of the spatial downscaling model are listed as following and the flow diagram is shown in Figure 2.

(1) The experimental data, including Landsat 8 OLI, SRTM DEM, land classification map, ASTER and MODIS LST product, were expected to registered to the same projection and then regions of study area were extracted to construct the standard datasets. The derived input variables were intended to be aggregated to the MODIS LST product with 990 m coarser resolution. In this study, the upscaling method is simply using the spatial averaging method. On this level, the statistical model between LST and other predictor variables could be established.

(2) The statistical model based on the coarser level can be expressed as following:

$$LST_c = F\left(\left(\rho_i\right)_c, \left(s_i\right)_c, \left(t\right)_c, \left(lc\right)_c\right) \tag{1}$$

where the subscript c means the variable with coarser resolution, subscript i represents the i-th variable, ρ is the reflectance, s represents the spectral indices, t represents the terrain factor and lc represents the land cover type. The function F $(\cdot)$ indicates a nonlinear regression model constructed between LST and these variables.

(3) There exists a residual temperature resulted from the difference between original and estimated LST, which is called model error, the formula is listed as following:

$$\Delta LST_c = LST_o - LST_c \tag{2}$$

where the subscript o represents the original LST.

(4) The statistical downscaling algorithms are commonly based on the assumption that there is a unique statistical relationship exists within a sensor scene at multiple spatial resolutions [5,9,17]. By introduction of predictor variables with finer resolution into the constructed model and allocation of model error, the downscaled LST product at finer resolution can be derived as following:

$$LST_f = F\left(\left(\rho_i\right)_f, \left(s_i\right)_f, \left(t_i\right)_f, \left(lc\right)_f\right) + \Delta LST_c \tag{3}$$

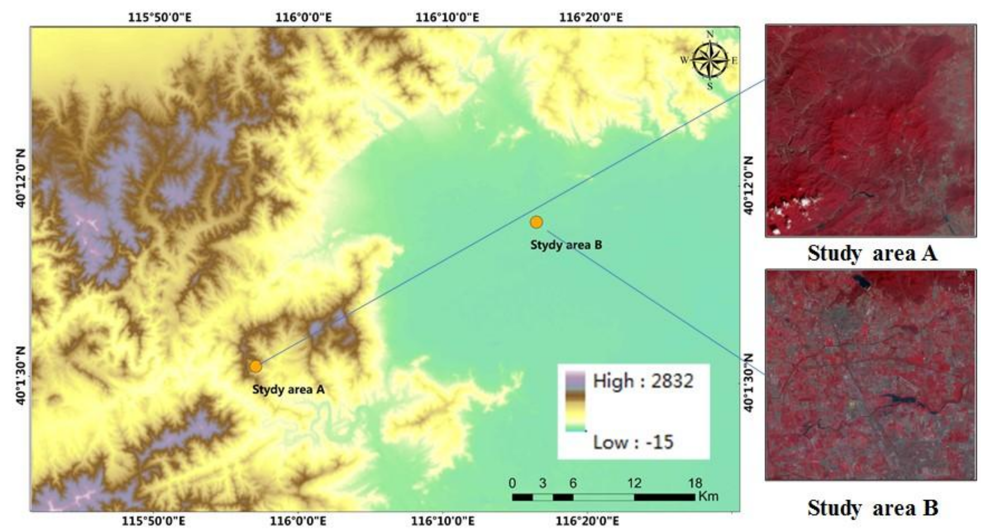

Figure 1. Geolocation of the study area in Beijing, China with elevation and false color images generated from Landsat 8 data (R: band 5; G: band 4; B: band 3). (a) study area A, (b) study area B.

2) Brief introduction of machine learning algorithms

Machine learning regression algorithms have been broadly utilized in remote sensing image processing, land cover classification and image sharping, which the superiority of high prediction accuracy and the rapid process of dealing with high dimensional data.

In this study, three rule-based machine learning algorithms, (ANN, SVM, and RF), were chosen in LST downscaling.

The ANN is a computing system constructed by an interconnected group of nodes and acquires knowledge through a learning process. Each node represents an interconnected neuron and the interconnection of weight which is repeatedly modified during training process represents the connection from the output of one artificial neuron to the input of another, the output of each node is computed by some non-linear function of the sum of its inputs. The ANN is suitable for solving problems such as non-deterministic reasoning with complex causality because of its self-learning, self-organization, error tolerance and excellent nonlinear approximation ability

[25-26]. In this study, training and test data were generated by random selection from dataset of two study areas, and the samples were divided by 70%, 15% and 15% of training, validation and testing, respectively.

The SVM, proposed by Cortes and Vapnik in 1995, is a popular machine learning algorithm in dealing with small-sample, nonlinear data and high-dimensional pattern recognition [27]. The basic concept of the SVM algorithm is based on the Vapnik-Chervonenkis Dimension theory and the principle of structural risk minimization. It seeks the best compromise between the complexity of model and the learning ability (that is, the ability to identify any sample without errors) based on the limited samples in order to obtain the best generalization ability of model [28]. More formally, the SVM serves as an ideal machine learning algorithm for classification and regression problems and has been successfully applied in different fields such as evapotranspiration estimation and precipitation estimation from remote sensing data [16]. In our study, the Gaussian radial basis function (RBF) is chosen as the kernel function of SVM, and the relevant parameters are penalty coefficient (C) and gamma, which are optimized by traversal to minimize the model error.

The RF is a new machine learning algorithm evolved from the bagging algorithm with the advantage of high accuracy and insensitivity to multi-collinearity [29-30]. As a nonlinear statistical ensemble regression method, the RF is ensembled by a set of uncorrelated classification and decision regression trees. The tree is based on the classification and regression trees (CART) algorithm, in which the basic concept is to construct a tree-like graph or model of decisions and their possible consequences by generating relative homogeneous subgroups by recursively partitioning the training dataset to the maximum variance between groups of independent variables and dependent variables in each of the terminal nodes of the tree [31]. The results of RF training turn out to be the voting output for all decision trees [31]. In our study, the key parameters of RF model are the number of decision trees and the maximum number of features to be split, which are optimized by traversal to minimize the model error.

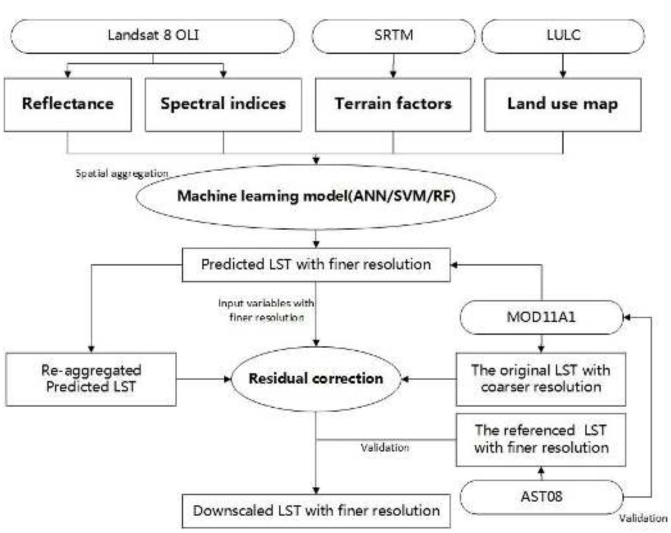

Figure 2. Schematic of the land surface temperature downscaling procedure by using machine learning algorithm.

III. Results and Analysis

A. *Downscaling performance in different surface conditions*

Three machine learning algorithms were applied to downscale the LST of MODIS products (the resampled resolution is 990m) to finer resolution with about 90m, and then the downscaled results were validated by ASTER LST products with 90m resolution. The root-mean square errors (RMSE) and the estimated biases are listed in Table 1 as following:

From Table 1 we can see, the average RMSE of three machine learning algorithms are about 2~3 K both in study area A and B, which perform the better results than that of TsHARP. The biases of these methods are almost close to zero, which means the unbiased estimation of machine leaning. The RF model achieves the most satisfied downscaled result with the RMSE of 2.22 K in study area A, about 0.6 K lower than TsHARP, following closely by that of ANN model, about 0.2 K lower than TsHARP; and also achieves the same satisfied result in study area B with the RMSE of 2.28 K, about 1.38 K lower than TsHARP, following by ANN and SVM, about 0.87 K and 0.56 K lower than TsHARP.

Figure 3 shows the error distribution boxplots of methods-processed LST derived by TsHARP and machine learning algorithms, which are more intuitional than the data graphs in Table 1. We can clearly draw the conclusion that the median of error is almost close to zero, which means the unbiasedness of algorithms. In Figure 3a, the box width of SVM and RF is ranged from about -1.5 to 1.5 K, narrower than that of TsHARP with the width limits about -3~3 K, this shows the more concentrated distribution of regression errors of SVM and RF. In addition, the outliers in TsHARP box seem to be much more than other algorithms. The similar conclusion could be reached in Figure 3b, in which the RF performs best with the smallest box width and the minimum outliers.

TABLE 1. RMSE AND BIAS OF DOWNSCALED LST IN DIFFERENT STUDY AREAS.

	Study area A		**Study area B**	
	RMSE	bias	RMSE	bias
TSHARP	3.22	0	3.66	0
ANN	2.62	-0.05	2.79	-0.2
SVM	2.82	-0.01	3.1	0.01
RF	2.22	0	2.28	-0.13

Figure 4c to 4f are the spatial distribution and Figure 6a to 6d are the error distribution of downscaled LSTs in study area A with several regression models. Compared with the spatial distribution of ASTER LST in Figure 4b, the spatial variance of 4c and 4f are apparently similar to the true LST products and the detailed information of land surface status are reserved completely. By introducing multiple type predictor variables, such as NDVI (which serves as a good indicator of vegetation coverage), land use map (which gives a classified reaction to

LST in different kinds of land surface) and the terrain factors including DEM, slope, aspect as well as hill-shade of mountains, the RF and ANN model depict the complicated terrain more precisely and completely. The SVM model, although performs slightly better than TsHARP with RMSE lower about 0.03 K, has made a smoothing effect on the spatial distribution of LST, thus a loft of spatial information is over looked, which performs slightly inferior to RF and ANN. The TsHARP model is based on the relationship between LST and vegetation index such as vegetation coverage, thus is more inclined to be affected by fitting residuals, which commonly leads to a misty texture feature. The lost information can be founded clearly form the Figure 3f especially in the sharp mountains.

The study area B, located in the downtown area in Beijing City, is mainly consist of the soaring skyscrapers and the bustling streets, together with consecutive road greening and continuous river. The complex land covers aggravate the spatial heterogeneity and the plenty of mixed pixels help reduce the accuracy of downscaling models. Therefore, the RMSE tested on study area B are almost higher than that in study area A, especially for TsHARP model, the single indictor towards LST. Similarly, the RF model gets the pretty steady regression results with the RMSE of 2.28 K, about 1 K lower than that of TsHARP. The difference of LST spatial difference and the error distribution of these downscaling algorithms in study area B is shown in Figure 5 and Figure 6d-6h, respectively. On the one hand, RF is insensitive to multicollinearity, which pledges the robustness of the result for missing and nonequilibrium data and has a satisfactory prediction for thousands of predictor variables. On the other hand, RF is a kind of ensemble algorithm integrated with many basic machines, the voting mechanism usually avoids the influence of outliers and get a desired result. The downscaled LST of SVM model in Figure 5e shows a more smoothing effect on land surface details, which shows a worse result than TsHARP.

From the above, the accuracies of downscaling results trained by ANN, SVM and RF seem to be similar to each other and all better than TsHARP. This conclusion has reinforced the superiority of machine learning. For further comparison, in terms of algorithm complexity, ANN and SVM are constructed by a number of complicated parameters which are sensitive to model training, while RF has the advantage of less parameters and simple algorithm, from this, the processing time of RF also seems to be much less than ANN and SVM. In addition, the smoothing effects that are not appeared in ANN and RF have weaken the downscaling performance of SVM, the reason is supposed to be the mechanism of SVM, which is more suitable for classification than regression.

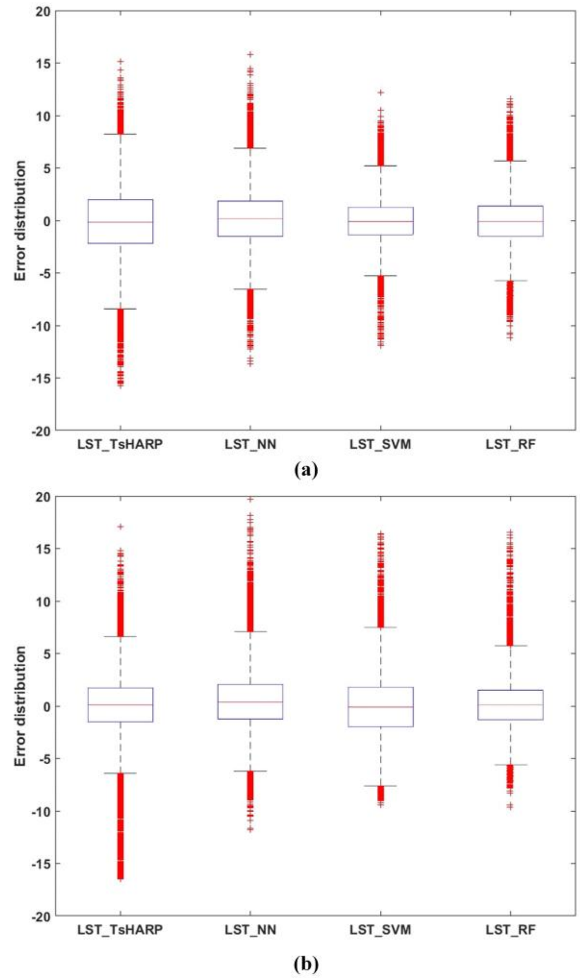

Figure 3. Comparison the error distribution of TsHARP LST, ANN LST, SVM LST and RF LST in (a) Study area A and (b) Study area B by box-plots.

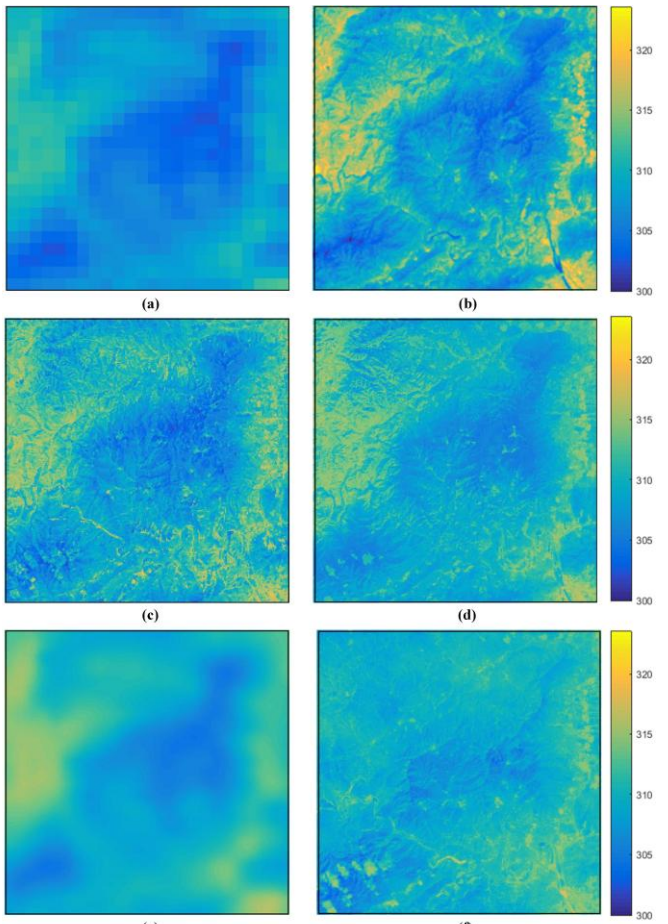

Figure 4. Spatial distribution of LSTs in study area A. (a) 990-m MODIS LST, (b) 90-m ASTER LST, (c) 90-m downscaled ANN LST, (d) 90-m downscaled RF LST, (e) 90-m downscaled SVM LST and (f) 90-m downscaled TsHARP LST.

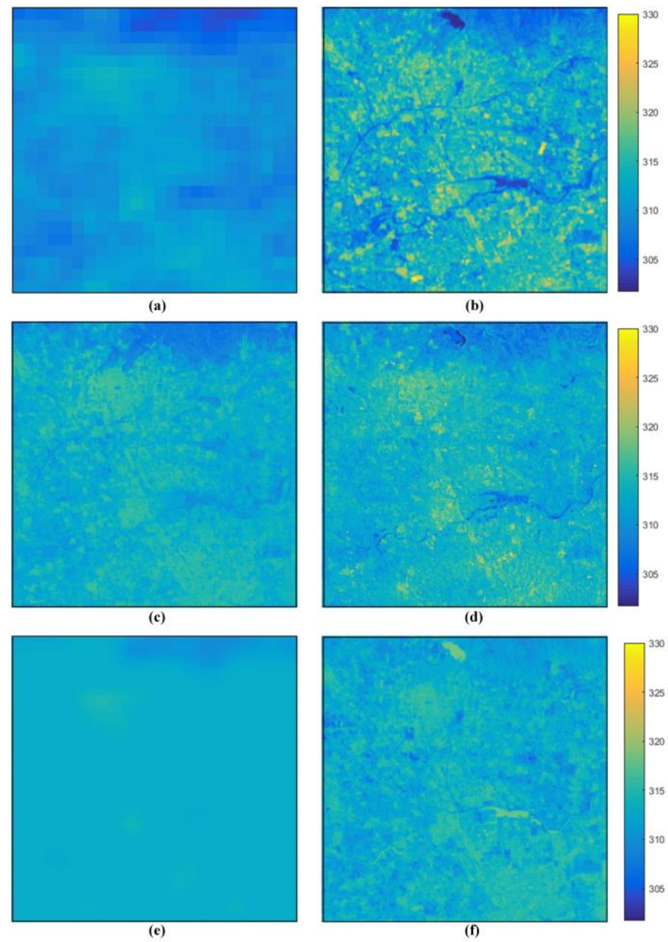

Figure 5. Spatial distribution of LSTs in study area B. (a) 990-m MODIS LST, (b) 90-m ASTER LST, (c) 90-m downscaled ANN LST, (d) 90-m downscaled RF LST, (e) 90-m downscaled SVM LST and (f) 90-m downscaled TsHARP LST.

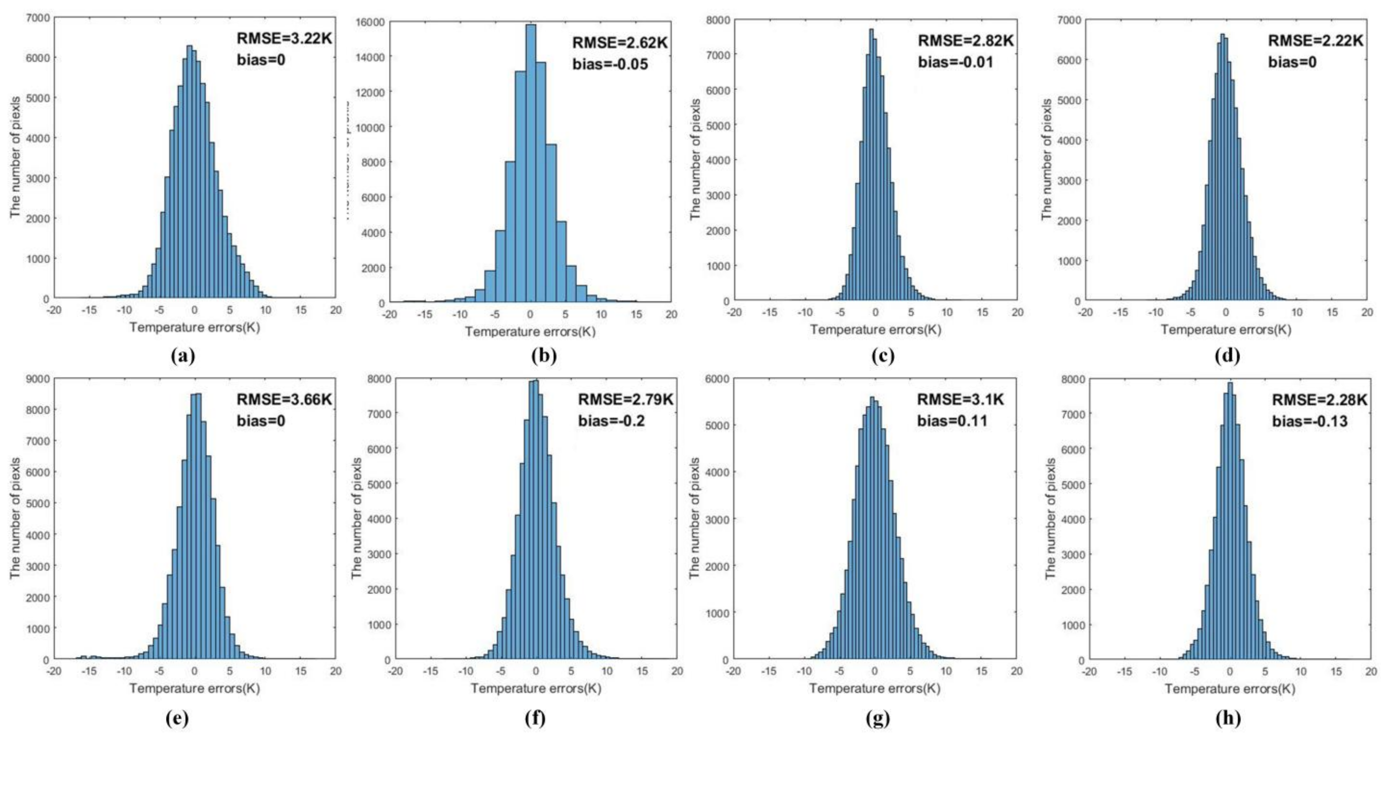

Figure 6. Distribution of LST errors between the estimated and reference LSTs (a) 90-m downscaled TsHARP LST for study area A,(b) 90-m downscaled ANN LST for study area A.(c) 90-m downscaled SVM LST for study area A.(d) 90-m downscaled RF LST for study area A. (e) 90-m downscaled TsHARP LST for study area B ,(f) 90-m downscaled ANN LST for study area B.(g) 90-m downscaled SVM LST for study area B.(h) 90-m downscaled RF LST for study area B.

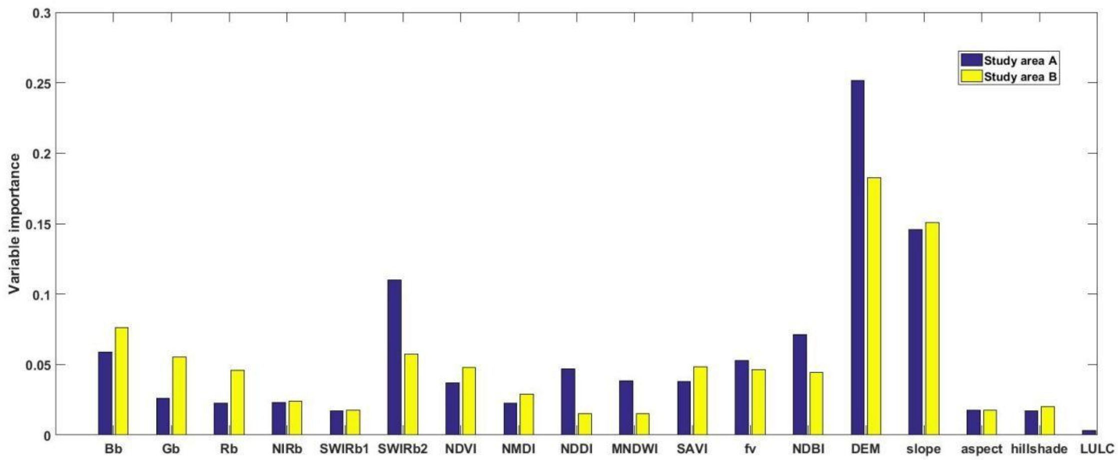

Figure 7. Random forest variable importance scores averaged across two study areas.

B. Variable Importance in Downscaling of LST

The RF algorithm provides measurements of variable importance. The resultant values are then used to rank the orderings of those independent variables in terms of their contribution to the regression model. Figure 7 shows the importance ranking of input variables calculated by RF algorithm in two study areas. Apparently, contributions of terrain factors, especially for DEM and slope are the highest in both of two areas. It implies that there are large topographic effects on the healing process for solar incident radiance in mountainous surface. Besides, the terrain-dominated study area A shows a significant inconsistency between DEM and other kind of variables, while the difference of importance scores in study area B seems to be not intensive because of the flat terrain. For study area A, largely covered by hills with the elevation ranging from 15~2832 m, the spatial distribution of LST would almost be controlled by these terrain factors and the vegetation fraction correlated factors. For study area B, the scene acquired at downtown area with the complicate landscapes and relatively flat terrain, DEM becomes less important than that in study area A. It's important to find that the importance ranking of NDVI in both two areas seems not more distinctive than other variables, which gives the further evidence that the NDVI-based algorithm, TsHARP would have a weak performance in regions with complex land cover type.

C. Downscaling results of the different training models

Downscaling algorithms trained on the specific area often reward with acceptable results because of the high correlation between training and testing data, which may give a concern about the overfitting problem of the model. For this reason, downscaling models trained on the study area A were applied the downscale the LST in study area B and vice versa. The statistical results of three machine learning algorithms and the TsHARP model are listed in Table 2. Compared the results in Tables 1, the regression accuracy of TsHARP are obviously declined with the RMSE increased about 0.43 K in study area A and 0.13 K in study area B. The same experiment were tested by other algorithms but the regression errors tend to be steady, and what is more amazing is that the RMSE of RF and ANN model with different training model and testing dataset appear to be (about 0.18 K of RF model and about 0.58 K of ANN model in study area A) lower than that of the same model and dataset, which give a strong evidence that the RF and ANN model are generalized enough to downscale LST using a different training model. Additionally, despite the lost spatial information and the smoothing effect of SVM, the RMSEs of SVM model are basically equal to the former result (about 0.14 K in study area A and 0.03 K in study area B), which also proves that the machine learning algorithms are strong enough to downscale LST with different training model.

TABLE 2. DOWNSCALING STATISTICS FOR VARIOUS REGIONS.

	Study area A using model B		**Study area B using model A**	
	RMSE	bias	RMSE	bias
TSHARP	3.65	0	3.79	-1.68
ANN	2.05	0.03	2.82	-0.01
SVM	2.96	-0.26	3.13	0.18
RF	2.04	0.03	2.3	-0.31

IV. CONCLUSION

In this study, three machine learning algorithms including ANN, SVM and RF model, were applied to downscale MODIS LST products from 990 m to 90 m. The case study was conducted over two typical study areas in Beijing; downscaled results were validated by the ASTER LST products with 90 m resolution and were compared with the common traditional downscaling algorithm - TsHARP. According to the results we can draw some conclusion as following:

Firstly, the model complexity of TsHARP model is far simpler than that of those machine learning algorithms, compared with ANN and SVM which have complex parameter optimization process, the RF model is lack of sensitivity to parameters, thus it has a relatively simple structure. Together with the number of input variables and computational complexity, the computation time of TsHARP is confirmed to be the least, followed by RF and ANN model, the SVM has the longest time with the most complicated mechanism. In terms of regression accuracy, machine learning algorithms are still superior to TsHARP model, no matter in areas with fully vegetation covered or in areas occupied with impervious surface. Especially for RF and ANN model, which shows more satisfied predicting effect with multiple type of predictor variables introduced. The SVM model, generally achieves a good result in number, but has a smoothing effect on land surface. Indeed, the NDVI-based TsHARP algorithm, with only one predictor variable into model, has an inadequate downscaling performance in areas with complicated land cover types.

The downscaling results in study area A are universally better than that of study area B. This is attached to the land cover types of study area. In the region with fully vegetation covered, the land cover types are relatively simple and the spatial distribution of LST are highly associated with DEM and vegetation index like NDVI, thus all algorithms even TsAHRP have received a good regression result. However, the downscaled LST did not adequately capture spatial variations in study area B, possibly due to the complex land surface combined with natural as well as artificial materials, which are more apt to derive mixed pixels. Thus, a more kinds of explanatory variable dataset needs to be established over regions with spatial heterogeneity.

One of the most significant advantages of machine learning algorithms is the robustness applied to different datasets using the trained model, this may be attribute to the introduction of multiple type predictor variables as well as the moderate model which depicts the nonlinear relationship between dependent variables and independent variables. In addition, RF provides with an indication for the selection of predictor variables in different kinds of regions. According to the variable importance measurements of the RF, DEM is the most significant variable, followed by slope, it means the great importance of terrain factors in downscaling LST. Moreover, the variable importance values in different regions would be reallocate following the different land cover types.

This study has provided thoughts in comparing the capacity and suitability of different machine learning algorithms in downscaling LST. Once the appropriate and adequate input variable dataset being constructed and the representative training samples of downscaling model being selected, the framework is expected to provide more precise LST products with high spatial and temporal resolution at the larger geographic context. In the future, further studies would be focused on the parameter optimization and process standardization of these machine learning algorithms to produce excellent quality LST products with high spatial resolution. Additionally, other land surface variables related to LST (such as soil moisture, humidity) could be introduced to examine whether these variables are beneficial for downscaling LST.

References

[1] Z.-L. Li, B.-H. Tang, H. Wu, H. Ren, G. Yan, Z. Wan, I. F. Trigo, and J. A. Sobrino, “Satellite-derived land surface temperature: Current status and perspectives,” Remote Sens. Environ., vol. 131, pp. 14–37, 2013.

[2] A. J. Arnfield, “Two decades of urban climate research: a review of turbulence, exchanges of energy and water, and the urban heat island,” Int. J. Climatol., vol. 23, no. 1. Papers, 1-26, 2003.

[3] V. Lakshmi, and D. Zehrfuhs, “Normalization and comparison of surface temperatures across a range of scales,” IEEE Trans. Geosci. Remote Sens., vol. 40, no. 12. Papers, 2636-2646, 2002.

[4] P. E. Dennison, K. Charoensiri, D. A. Roberts, S. H. Peterson, and R. O. Green, “Wildfire temperature and land cover modeling using hyperspectral data,” Remote Sens. Environ., vol. 100, no. 2. Papers, 212-222, 2006.

[5] W. P. Kustas, J. M. Norman, M. C. Anderson and A. N. French, “Estimating subpixel surface temperatures and energy fluxes from the vegetation index–radiometric temperature relationship,” Remote Sens. Environ., Papers, 85(4):429-440, 2003.

[6] L. J. Guo, and J. M. Moore, “Pixel block intensity modulation: Adding spatial detail to TM band 6 thermal imagery,” Int. J. Remote Sens., vol. 19, no. 13. Papers, 2477-2491, 1998.

[7] B. Zhukov, D. Oertel, F. Lanzl and G. Reinhackel, “Unmixing-based multisensor multiresolution image fusion,” IEEE Trans. Geosci. Remote Sens., vol. 37, no. 3. Papers, 1212-1226 , 1999.

[8] A. Dominguez, J. Kleissl, J. C. Luvall, “High-resolution urban thermal sharpener (HUTS),” Remote Sens. Environ., Papers,115(7):1772-1780, 2011.

[9] N. Agam, W. P. Kustas, M. C. Anderson, F. Li, and C. M. U. Neale “A vegetation index based technique for spatial sharpening of thermal imagery,” Remote Sens. Environ., vol. 107, no. 4. Papers, 545-558, 2007.

[10] K. Zakšek, K. Oštir, “Downscaling land surface temperature for urban heat island diurnal cycle analysis,” Remote Sens. Environ., Papers,117, 114–124, 2012.

[11] J.J. Qu, X. Hao, M. Kafatos, L. Wang, “Asian dust storm monitoring combining Terra and Aqua MODIS SRB measurements,” IEEE Geosci. Remote Sens. Lett., Papers, 3, 484–486, 2006.

[12] S. B. Duan and Z. L. Li, "Spatial Downscaling of MODIS Land Surface Temperatures Using Geographically Weighted Regression: Case Study in Northern China," IEEE Trans. Geosci. Remote Sensing, vol. 54, no. 11, pp. 6458-6469, 2016.

[13] S. Mukherjee, P. K. Joshi, and R. D. Garg, "Regression-Kriging Technique to Downscale Satellite-Derived Land Surface Temperature in Heterogeneous Agricultural Landscape," IEEE Journal of Selected Topics in Applied Earth Observations & Remote Sensing, vol. 8, no. 3, pp. 1245-1250, 2015.

[14] D. Fasbender, D. Tuia, P. Bogaert, and M. Kanevski, "Support-Based Implementation of Bayesian Data Fusion for Spatial Enhancement: Applications to ASTER Thermal Images," IEEE Geoscience & Remote Sensing Letters, vol. 5, no. 4, pp. 598-602, 2008.

[15] F.S. Mpelasoka, A.B. Mullan, R.G. Heerdegen, “New Zealand climate change information derived by multivariate statistical and artificial neural networks approaches,” Int. J. Climatol., Papers, 21, 1415–1433, 2001.

[16] J.A. Gualtieri, S. Chettri, “Support Vector Machines for classification of hyperspectral data,” In Proceedings of the IGARSS 2000., Papers, 813–815, 2000.

[17] C. Hutengs, M. Vohland, “Downscaling land surface temperatures at regional scales with random forest regression,” Remote Sens. Environ., Papers, 178, 127–141, 2016.

[18] Y. Yang, X.L. Li, C. Cao, “Downscaling urban land surface temperature based on multi-scale factor,” Science of Surveying & Mapping, 2017.

[19] W. F. Zhan, Y. H. Chen, J. Zhou, J. F. Wang, W. Y. Liu, James Voogt, X. L. Zhu, J. L. Quan, J. Li, "Disaggregation of remotely sensed land surface

temperature: Literature survey, taxonomy, issues, and caveats," Remote Sens. Environ., vol. 131, no. 8, pp. 119-139, 2013.
[20] M. Bisquert, J. M. Sanchez, and V. Caselles, "Evaluation of Disaggregation Methods for Downscaling MODIS Land Surface Temperature to Landsat Spatial Resolution in Barrax Test Site," IEEE Journal of Selected Topics in Applied Earth Observations & Remote Sensing, vol. 9, no. 4, pp. 1430-1438, 2016.
[21] S. Bonafoni, "Downscaling of Landsat and MODIS Land Surface Temperature Over the Heterogeneous Urban Area of Milan," IEEE Journal of Selected Topics in Applied Earth Observations & Remote Sensing, vol. 9, no. 5, pp. 2019-2027, 2016.
[22] Z.M. Wan, J. Dozier, “A generalized split-window algorithm for retrieving land-surface temperature from space”. IEEE Trans. Geosci. Remote Sens., 34, 892-905, 1996.
[23] A. Gillespie, S. Rokugawa, T. Matsunaga, J. S. Cothern, S. Hook, A. B. Kahle, “A temperature and emissivity separation algorithm for Advanced Spaceborne Thermal Emission and Reflection Radiometer (ASTER) images,” `EEE Trans. Geosci. Remote Sens., 36, 1113-1126, 2002.
[24] W. Zhan, Y. Chen, J. Zhou, “Sharpening Thermal Imageries: A Generalized Theoretical Framework From an Assimilation Perspective,” IEEE Trans. Geosci. Remote Sens., Papers, 49(2):773-789, 2011.
[25] G. S. Dwarakish, S. Rakshith, U. Natesan, "Review on Applications of Neural Network in Coastal Engineering," Artificial Intelligent Systems and Machine Learning., 5 (7): 324–331, 2013.
[26] L. Ermini, F. Catani, N. Casagli, “Artificial Neural Networks applied to landslide susceptibility assessment,” Geomorphology, 66(1):327-343, 2005.
[27] C. Cortes and V. Vapnik, "Support-vector networks," Machine Learning, vol. 20, no. 3, pp. 273-297, 1995.
[28] W. Jing, Y. Yang, X.F. Yue, X.D. Zhao, “A Comparison of Different Regression Algorithms for Downscaling Monthly Satellite-Based Precipitation over North China,” Remote Sens., 8(10):138-144, 2016.
[29] L. Breiman, “Random forests, machine learning 45,” J. Clin. Microbiol., Papers, 2:199-228, 2001.
[30] Y. Yang, C. Cao, X. Pan, “Downscaling Land Surface Temperature in an Arid Area by Using Multiple Remote Sensing Indices with Random Forest Regression,” Remote Sens., Papers, 9(8), 2017.
[31] L. Breiman, J. H. Friedman, R. A. Olshen, C. J. Stone, “Classification and Regression Trees. Chapman et. Classification and regression trees,” Wadsworth International Group, 243-6, 1984.
[32] T. G. Dietterich, “An Experimental Comparison of Three Methods for Constructing Ensembles of Decision Trees: Bagging, Boosting, and Randomization,” Mach. Learn., Papers, 40(2):139-157, 2000.

Wan Li received B.S. degree in geographical condition monitoring from Wuhan University, Wuhan, China, in 2012. She is currently pursuing the M.S. degree cartography and geographical information system from the Institute of Geographic Sciences and Natural Resources Research, Chinese Academy of Sciences, Beijing, China, in 2018. Her research interests include the scale transformation of land surface temperature.

Li Ni received the B.S. degree and the M.S. degree in photogrammetric engineering and remote sensing from Wuhan University, Wuhan, China, in 2003 and 2006, respectively. She is currently pursuing the Ph.D. degree in cartography and geographical information system at Center for Earth Observation and Digital Earth, Chinese Academy of Sciences. She is currently an Associate Research Fellow with Key Laboratory of Digital Earth Science, Institute of Remote Sensing and Digital Earth, Chinese Academy of Sciences. Her research interests focus on the hyperspectral remote sensing.

Hua Wu received the B.S. degree in photogrammetric engineering and remote sensing from Wuhan University, Wuhan, China, in 2003, the M.S. degree in cartography and geographical information system from Beijing Normal University, Beijing, China, in 2006, and the Ph.D. degree in cartography and geographical information system from the Institute of Geographic Sciences and Natural Resources Research, Chinese Academy of Sciences, Beijing, in 2010.

He is currently an Associate Research Fellow with the Institute of Geographic Sciences and Natural Resources Research, Chinese Academy of Sciences. His research mainly includes the retrieval, validation, and scaling of remotely sensed products.

Zhao-Liang Li received the Ph.D. degree in 1990. Since 1992, he has been a research scientist at CNRS, Illkirch, France. He joined the Institute of Agricultural Resources and Regional Planning in 2013. He has participated in many national and international projects such as NASA-funded MODIS, EC-funded program EAGLE, and ESA funded programs SPECTRA, etc. His main expertise fields are in thermal infrared radiometry, parameterization of land surface processes at large scale, as well as in the assimilation of satellite data to land surface models. He has published more than 100 papers in international refereed journals.

Si-Bo Duan received the Ph.D. degree in cartography and geographical information system from the Institute of Geographic Sciences and Natural Resources Research, Chinese Academy of Sciences, Beijing, China, in 2014. He is currently a Associate Research Fellow with the Institute of Agricultural Resources and Regional Planning, Chinese Academy of Agricultural Sciences. His research interests include the retrieval and validation of land surface temperature.